

DESY SR-76/05  
March 1976

Performance of a High Resolution Monochromator for the  
Vacuum Ultraviolet Radiation from the DORIS Storage Ring

by

DESY-Bibliothek,  
24. MRZ. 1976

V. Saile, M. Skibowski, W. Steinmann  
*Sektion Physik der Universität München*

P. Gürtler  
*II. Institut für Experimentalphysik, Universität Hamburg*

E. E. Koch and A. Kozevnikov  
*Deutsches Elektronen-Synchrotron DESY, Hamburg*

To be sure that your preprints are promptly included in the  
HIGH ENERGY PHYSICS INDEX ,  
send them to the following address ( if possible by air mail ) :

DESY  
Bibliothek  
2 Hamburg 52  
Notkestieg 1  
Germany

Performance of a High Resolution Monochromator for the  
Vacuum Ultraviolet Radiation from the DORIS Storage Ring<sup>+</sup>

by

V. Saile<sup>(a)</sup>, P. Gürtler<sup>(b)</sup>, E.E. Koch<sup>(c)</sup>, A. Kozevnikov<sup>(c)</sup>§  
M. Skibowski<sup>(a)++</sup>, and W. Steinmann<sup>(a)</sup>

(a) Sektion Physik der Universität München, 8 München 40

(b) II. Institut für Experimentalphysik, Universität Hamburg, 2 Hamburg 52

(c) Deutsches Elektronen-Synchrotron DESY, 2 Hamburg 52

*The unique properties of the DORIS storage ring at DESY as a synchrotron radiation source are exploited for high resolution spectroscopy in the vacuum ultraviolet. We describe a new experimental set up with a 3 meter normal incidence monochromator for wavelengths between 3000 Å to 300 Å ( $4 \leq h\nu \leq 40$  eV) using a vertical dispersion plane. The storage ring provides a light flux intense and stable enough for rapid photoelectrical scanning of the spectra with a resolution of 0.03 Å in first order.*

---

<sup>+</sup> Work supported in part by Deutsche Forschungsgemeinschaft DFG and Bundesministerium für Forschung und Technologie BMFT

§ permanent address: Institut für Kernphysik, Tomsk, UdSSR

++ now at Universität Kiel

## 1. Introduction

Optical spectroscopy in the Vacuum Ultraviolet (VUV) spectral region (2000 Å to 2 Å) has profited immensely by the outstanding properties of synchrotron radiation from electron accelerators and storage rings. Synchrotron radiation provides a continuous spectrum from the infrared over the visible, the UV and VUV far into the X-ray region.<sup>1</sup> It is now the most powerful light source available for spectroscopy at wavelengths below 2000 Å. In particular the use of synchrotron radiation from high current storage rings makes possible a number of experiments with extreme requirements as regards intensity and stability of the light source. However, the adaptation of an experiment to such a light source is not an easy matter.

In this paper we describe the layout and performance of a new experimental set up for the spectral range 3000 - 300 Å with a 3m normal incidence monochromator. With this apparatus the unique properties of the DORIS storage ring as a synchrotron radiation source<sup>2</sup> are exploited for high resolution spectroscopy. A resolution of 0.03 Å in first order with a 1200 1/mm grating is obtained, while at the same time the intensity and stability is excellent and high enough for rapid photoelectrical scanning of the spectra.

## 2. Experimental Arrangement

### 2.1 The source

The DORIS electron-positron storage rings at DESY provide synchrotron radiation of a high degree of collimation and intense continuous spectral distribution from the infrared out to X-ray wavelengths. Furthermore the light is highly polarized and has a time structure with pulses as short as 0.2 nsec. These properties and the general layout of the new laboratory for synchrotron radiation at the DORIS storage ring have been described in detail recently.<sup>2</sup>

In Fig. 1 the data relevant for the optical design and performance of the high resolution monochromator are shown. The number of photons per  $\text{\AA}\cdot\text{sec}$  impinging on the premirror 35 m away from the source point which are available for the monochromator is given in the upper part. Under typical operation conditions of the storage ring (1.75 GeV, 200 mA)  $1.5 \times 10^{13}$  photons per eV and sec are available at 20 eV. The degree of polarization  $P = \frac{I_{\parallel} - I_{\perp}}{I_{\parallel} + I_{\perp}}$ , where  $I_{\parallel}$  and  $I_{\perp}$  are the intensities for the components polarized parallel and perpendicular to the orbital plane of the electrons in the storage ring, is shown for  $h\nu = 10$  eV (and 3.5 GeV electron energy) in the middle part of Fig. 1 as a function of elevation angle  $\psi$  against the orbital plane. For practical purposes it is interesting to note that typical storage times of the electron beam are presently 8 to 12 hours during which the circulating electron current decreases from about 300 mA to 100 mA (see lower part of Fig. 1).

## 2.2 Optical design

The beam line including the optical components is schematically sketched in Fig. 2. Synchrotron light emitted tangentially from the electron orbit in the storage ring passes through an ultra high vacuum (UHV) beam pipe over a distance of about 35 m towards a beam splitter (PMC). This is a plane mirror (330x65 mm reflecting area) which reflects part of the light with a cross section of 4 cm width, 5 cm height horizontally out of the direct beam under an angle of incidence of  $82.5^{\circ}$ . Subsequently the light beam is reflected upwards under an angle of incidence of  $82.5^{\circ}$  and focused by a toroidal mirror (TM) (500x50 mm reflecting area) in a second mirror chamber (TMC) onto the horizontal entrance slit (S) of the monochromator with a vertical dispersion plane. The radii of curvature for this toroidal mirror are  $R_1 = 28\,980$  mm

within the plane of dispersion of the monochromator and 494 mm perpendicular to it. The monochromatic beam emerges from the exit slit (S) horizontally.

The vertical mounting of the instrument offers several advantages: firstly the vertical extension of the electron beam within the storage ring is smaller ( 1 mm) than the horizontal extension ( 10 mm). Optimum focusing conditions for the 3 m instrument preserves the relation of 1:10 for height to width of the beam size at the entrance slit and consequently the mounting with horizontal slits matches the source geometry. Secondly, the reflections at the optical components (with exception of the plane premirror) always occur with the main component of the electric field vector of the light parallel to the surface (perpendicular to the plane of incidence), thus presumably always enhancing the degree of polarization. In this way optimum intensity and a high degree of polarization is available for the experiments at the exit slits.

Special attention has been given to the choice of reflecting mirrors which can withstand the intense synchrotron radiation. For the plane premirror Zerodur, a glass ceramic material<sup>3</sup> is now successfully used over a 6 months period. This material has an expansion coefficient of  $2 \times 10^{-8}$  per degree °C up to 300° C and thus a very good mechanical stability. So far the intense radiation did not change the optical performance of this mirror. Alternatively a steel mirror with chromium coating can be used.<sup>4</sup> This mirror has not yet been tested over a long term period. Both mirrors have a surface roughness of  $\leq 10 - 20 \text{ \AA}$ .

### 2.3 Monochromator

The 3m normal incidence VUV scanning monochromator is a special UHV-version of the McPherson model 225.3 modified to the requirements in the DORIS

synchrotron radiation laboratory according to our specification. The dispersion plane of the instrument is turned by  $90^\circ$  with respect to the standard orientation thus offering the advantages as mentioned in section 2.2. The total angle between the beams is fixed at  $15^\circ$  and provides adequate spacing for mounting accessories directly behind the slits. The monochromator incorporates the patented McPherson type optical system<sup>5</sup> that automatically positions the grating for focus over the entire wavelength range while the beam and slits remain in fixed positions.

The instrument covers a mechanical wavelength range from central image (zero order) to  $3000 \text{ \AA}$  with a standard  $1200 \text{ l/mm}$  grating installed. This grating provides a reciprocal linear dispersion of approximately  $2.8 \text{ \AA/mm}$ . An extra large grating housing allows installation of large gratings. The maximum size compatible with the housing is  $76 \times 160 \times 25 \text{ mm}$  blank size. The entrance and exit slit assemblies contain three slits of  $10\mu$ ,  $50\mu$  and  $100\mu$  width each one  $1 \text{ cm}$  long. Each of the slits can be brought into position under vacuum conditions. The precision ball screw sine drive assembly for the wavelength scan is driven by a special stepping drive controller. Wavelength scan control is achieved via a shaft extension to an encoder with  $1000$  steps per  $\text{\AA}$ . The shaft is connected to the precision ball screw by a rotary feedthrough. Wavelength scan control, scan speed control ranging from  $0.5 \text{ \AA/minute}$  to  $2500 \text{ \AA/minute}$  and digital wavelength display in  $\text{nm}$  units is provided in one electronic unit (McPherson Model 785  $\text{\AA}$  scan controller).

#### 2.4 Alignment

The alignment of the whole optical system has four steps. Independent supports for all components make a step by step procedure possible. First the plane premirror is adjusted with its plane of incidence parallel to the plane of the storage ring. Secondly the toroidal mirror defining the dis-

persion plane and the position of the entrance slit is aligned. It can be rotated with the aid of precision screws around any axis through the center of the reflecting surface. The most critical alignment is the deflection upwards out of the plane of the storage ring in order to bring the focus onto the entrance slit. It is achieved by a shaft extension and a linear feed-through and can be readjusted after bakeout under UHV-conditions. In a third step the entrance slit of the monochromator is brought into the focus of the toroidal mirror. This independent alignment can be performed under UHV conditions by sliding the whole monochromator on a plane inclined by  $15^\circ$  with respect to the floor. Viewing ports at the monochromator slits for observation of the front and rear of the entrance and exit slit respectively considerably facilitate alignment. The final adjustment of the experimental chamber is a straight forward routine.

## 2.5 Vacuum and mechanical assembly

Ultra high vacuum free of hydrocarbons in the beam pipe system, the mirror chambers and the monochromator is mandatory for avoiding surface contaminations on the mirrors and grating. All-metal UHV components and metal seals are used throughout the system, including the monochromator. After roughing with turbo molecular pumps a pressure of  $1 \times 10^{-9}$  Torr or better is maintained with ion pumps in the beam pipe system and the mirror chambers,  $2 \times 10^{-9}$  Torr within the monochromator housing and a pressures ranging from  $1 \times 10^{-1}$  to  $1 \times 10^{-1}$  Torr in the experimental chamber. Due to the heavy metal construction for the supports (Fig. 2) and thanks to the fact that the vacuum is maintained by ion pumps, we encountered no problems with vibrations even when the 10 $\mu$  slits were used.



## 2.6 Sample chamber and experimental equipment

In the first experiments with the new instrument an UHV-experimental chamber (EC in Fig. 2) with 450 mm diameter and a height of 450 mm was used. Pressures in the low  $10^{-11}$  Torr range can be achieved. With a turbo molecular roughing pump and a 400 l/sec ion pump with integrated sublimation pump and a  $N_2$ -cryopenal. For absorption experiments we used a bakeable UHV gas handling system. For these measurements the ion pump unit can be separated from the main experimental chamber by a valve. For optical experiments on solids and solidified gases the UHV experimental chamber can be equipped with a He-flow cryostat and reflectometer, an electrostatic bakeable detector being incorporated.

## 3. Operation and Performance

During the first weeks of operation we have checked the performance of the instrument in a number of experiments as regards the stability of the set up, the accuracy of calibration, spectral distribution and the intensity of the light flux and the resolution obtainable with the instrument. In this section we present some first results which demonstrate the great capability of the new system.

The wavelength of the instrument was calibrated with the well known rare gas resonance lines<sup>6</sup> and absorption lines of  $N_2$ ,  $H_2O$  and  $D_2O$  measured previously under very high resolution<sup>7-11</sup>. An absolute reproducibility of 0.2 Å could be obtained for the wavelength readings. When the central image was checked before each run the readings remained reproducible within 0.1 Å.

Figure 4 shows the continuous spectral distribution between 500 and 2000 Å behind the exit slit of the monochromator, measured with a sodium salicylate screen and a photomultiplier (EMI 9804/A). The spectrum is determined by the

intensity distribution of the light incident on the grating, the grating efficiency and the quantum efficiency of the detection system. Figure 4 shows the combined influence of these factors: the intensity per wavelength interval of the incident radiation still increases with decreasing wavelength in this spectral region, the grating yield determined mainly by the blaze and the reflectivity of the reflecting surface peaks at about 1200 Å. The sensitivity of the fluorescent screen-photomultiplier combination is almost constant in this range.<sup>12</sup> From our previous experience with other gratings we anticipate that we shall obtain useful intensity down to 300 Å with Au or Pt coatings and a blaze at shorter wavelength.

Absolute intensities at the exit slit of the monochromator have been determined with a double ionization chamber of the Samson type.<sup>13</sup> At 1200 Å, corresponding to 10.33 eV a photon flux of  $6 \times 10^9$  photons/0.3 Å\*sec has been measured with 100 $\mu$  slit width (corresponding to a 0.3 Å wavelength interval) under typical operating conditions of the storage ring (1.8 GeV and 200 mA stored electron beam). Reduction of the slit widths to 50 $\mu$  and 10 $\mu$  resulted in measured photon fluxes per resolution interval at 200 mA of  $1 \times 10^9$  photons / 0.15 Å x sec and  $2 \times 10^7$  photons / 0.03 Å x sec respectively. These numbers compare favourably with those calculated on the basis of the intensity of the radiation (Fig. 1), taking into account (i) the losses by reflections at the premirrors with 80 % reflectivity, (ii) an estimated grating efficiency of 7 % and (iii) a geometrical factor for the fact that presently the ruled area of the grating is only one third of the illuminated area. Such an estimate yields  $3 \times 10^{10}$  photons / Å sec. This number, when compared to the actual photon flux of  $2 \times 10^{10}$  photons / Å sec indicates the excellent performance of the whole optical system, including in particular the good focusing properties of the toroidal mirror.

Figure 5 demonstrates the resolution and quality in case of an atomic absorption spectrum, namely the Beutler-Fano absorption lines of  $\text{Kr}^{14+}$  in the VUV. The spectrum was obtained with a Kr-pressure of  $5 \times 10^{-3}$  Torr in the absorption chamber and a path length of 55 cm. The pressure in the monochromator remained in the  $10^{-9}$  Torr range. Figure 5 is a direct reproduction from the original strip chart recording demonstrating the quality and high resolution which can be achieved. It shows two series of autoionization lines converging to the  $^2P_{1/2}$  state of the  $\text{Kr}^+$  ion, namely  $4p^6 \rightarrow 4p^5nd'$  and  $4p^6 \rightarrow ns'$ , respectively, where the lower members of these series are not displayed. Note that one can follow the series up to  $n=25$  and  $n=35$  for the  $s'$  and the  $d'$  series respectively and that fine structure within the  $s'$ -lines (e.g.  $n=13s'$ ) is resolved.<sup>17</sup> Furthermore at the series limit 3 absorption maxima and 2 minima fall into a  $0.05 \text{ \AA}$  wavelength interval. This spectrum as well as spectra of Ar and Xe compare very favourably to spectra recently obtained with a 10 m spectrograph and a BRV-continuum light source.<sup>18</sup>

In Fig. 6 part of the  $\text{N}_2$  absorption spectrum is reproduced which represents only a small fraction ( $\approx 1/25$ ) of the structured absorption spectrum between 12 and 17 eV. Again a direct reproduction from the original strip chart recording is shown. In this case we were able to resolve the rotational structure of the individual vibrational bands (for the assignments see Ref. 11). The amount of detailed information obtainable is evident from the figure.

The high resolution and stability of the instrument was also exploited in a series of measurements on exciton bands in solids. In particular a precise line shape analysis and a detailed study of the temperature dependence of exciton lines, their splittings and shifts, was carried out with an accuracy not yet achievable with other set ups for this spectral range<sup>19</sup>.

#### 4. Conclusions

Following the first period of measurements with the new high resolution monochromator a number of improvements are under way: (1) use of differently blazed and coated gratings for an extension of the spectral region to shorter wavelength, (2) use of larger, eventually holographically produced gratings for an increase of the photon flux, (3) installation of a focusing mirror behind the exit slit for a reduction of the beam size at the sample, (4) direct connection of the monochromator and experiment to a PDP 11/45 computer for fast data acquisition and evaluation.

Although several spectrographs with larger focal length are available, with which spectra can be photographed at higher orders with even better resolution, the new system described here offers decisive advantages for spectroscopy on gases, molecules and solids in the VUV, for example:

1. Rapid photoelectric scanning over large photon energy ranges.
2. Determination of oscillator strength and line shapes with high resolution and with high accuracy due to photoelectric recording.
3. Investigation of secondary processes such as photoelectron emission, luminescence and fragmentation requiring tunable photon energies and high resolution.

Acknowledgement

The generous financial support from DFG and BMFT is gratefully acknowledged. One of us (A.K.) wishes to thank the Deutsche Forschungsgemeinschaft for support for a one year's visit of the DESY synchrotron radiation group. We thank B. Fancy (GCA McPerson) for his efficient help during the set up period. Thanks are also due to E.W. Schlag (TU München) for his encouraging interest in this project. Finally this work profited from the advice and help obtained in discussions with several members of the synchrotron radiation group at DESY.

## References

1. For a recent discussion of the use of synchrotron radiation as a light source see: C. Kunz, Perspectives of Synchrotron Radiation, in: Vacuum Ultraviolet Radiation Physics, edited by E.E.Koch, R. Haensel and C. Kunz, Pergamon-Vieweg, Braunschweig 1974, p. 753
2. E.E. Koch, C. Kunz and E.W. Weiner, The Synchrotron Radiation Laboratory at the DESY Storage Ring DORIS, Optik (1976) in press
3. Registered trade name of Schott and Gen., Mainz; manufactured by Carl Zeiss, Oberkochen
4. Manufactured by Leitz, Wetzlar
5. US Patent Nr. 3,090,863
6. C.E. Moore, Atomic Energy Levels, NBS Circular 467, Nat.Bur.Stand. 35/V.I Dec. 1971
7. P.K. Carroll, J.Chem.Phys. 58, 3597 (1973)
8. V. Carter, J.Chem.Phys. 56, 4195 (1972)
9. J.W.C. Johns, Canad.J.Phys. 41, 209 (1963)
10. A.E. Douglas, High Resolution Vacuum Ultraviolet Spectroscopy of Diatomic Molecules, in: Chemical Spectroscopy and Photochemistry in the Vacuum-Ultraviolet, edited by C. Sandorfy, P.J. Ausloos and M.B. Robin, D. Reidel Publ. Comp. Dordrecht (1974) p. 113
11. K. Dressler, Can.J.Phys. 47, 547 (1969)
12. E.C. Bruner, J.Opt.Soc.Am. 59, 204 (1969)
13. J.A.R. Samson, Techniques of Vacuum Ultraviolet Spectroscopy, Wiley, New York 1967
14. H. Beutler, Z. Phys. 93, 177 (1935)
15. R.E. Huffman, Y. Tanaka, J.C. Larrabee, J.Chem.Phys. 39, 902 (1963)
16. V. Carter and R.D. Hudson, J.Opt.Soc.Am. 63, 733 (1973)

17. P. Gürtler, E.E. Koch, A. Kozevnikov and V. Saile, to be published
18. E. Boursey and H. Damany, *Appl. Optics* 13, 589 (1974)
19. V. Saile et al., to be published

## Figure Captions

Fig. 1 Upper part: Spectral distribution of intensity impinging on the pre-mirror in a window  $40 \times 50$  mm in a distance of 35 m from the source point for two energies of the stored electron beam. Middle: degree of linear polarization as a function of elevation angle for 10 eV photon energy and 3.5 GeV electron energy. Lower part: decrease of the stored electron current with operating time.

Fig. 2 Schematic drawing of the beam pipe and the 3 m normal incidence monochromator cut perpendicular to the storage ring plane. Synchrotron radiation (SR) enters from the left, is deflected  $15^\circ$  out of its direction by a plane mirror in the mirror chamber PMC and reflected upwards  $15^\circ$  and focused by the toroidal mirror TM in the TM-chamber TMC onto the entrance slit (S) of the monochromator (225.3 D). It hits the grating (G). A monochromatic beam emerges horizontally from the exit slit (S) into the experimental chamber (EC). V = valve.

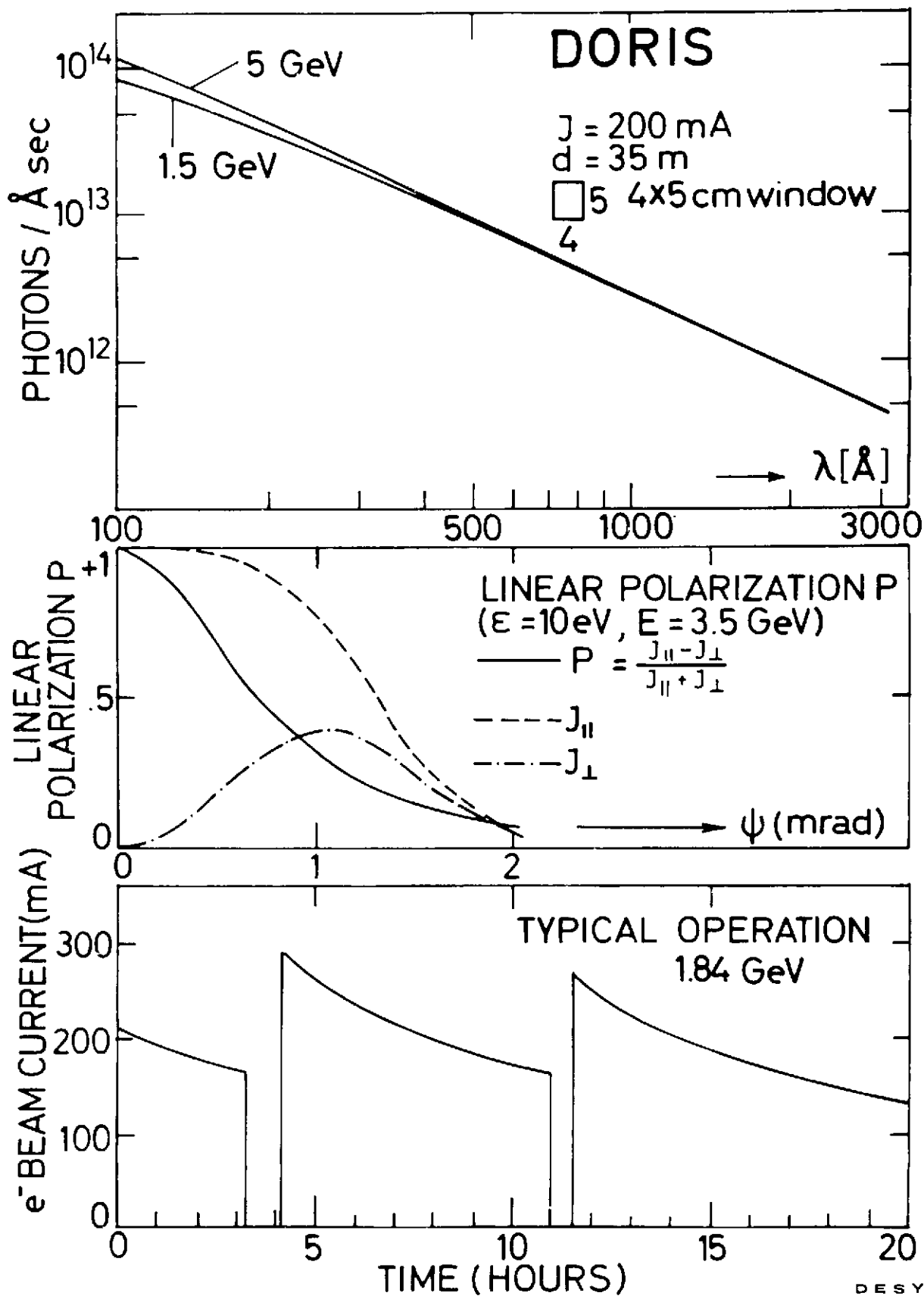
Fig. 3 Photograph of the instrument. For details see the description of Fig. 2. The straight beam line as well as the pumping unit for the experimental chamber can also be seen.

Fig. 4 Intensity of the photon flux available at the exit slit of the monochromator when a 1200 l/mm grating blazed at  $1350 \text{ \AA}$  with Al and  $\text{MgF}_2$  coating is used (1.8 GeV and 200 mA).



Fig. 5 Absorption spectrum of Kr in the region of the  $4p^6 \rightarrow 4p^5 ns', nd'$  autoionization. An original stripchard recording is reproduced.

Fig. 6 Absorption spectrum of  $N_2$  showing three vibrational bands at around  $960 \text{ \AA}$ . An original stripchard recording is reproduced. For the assignments see Ref. 9.



DESY

24359

Fig. 1

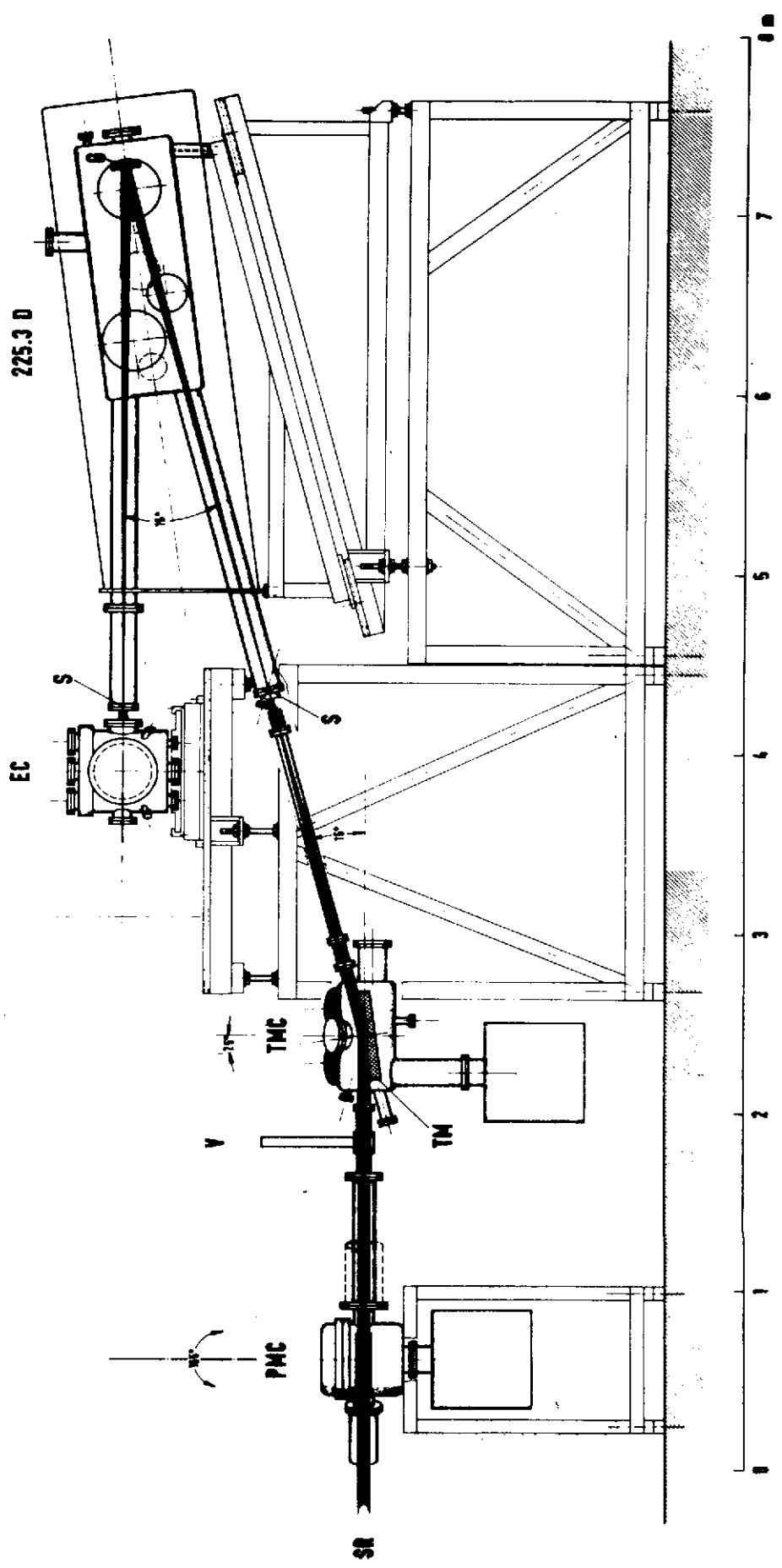


Fig. 2

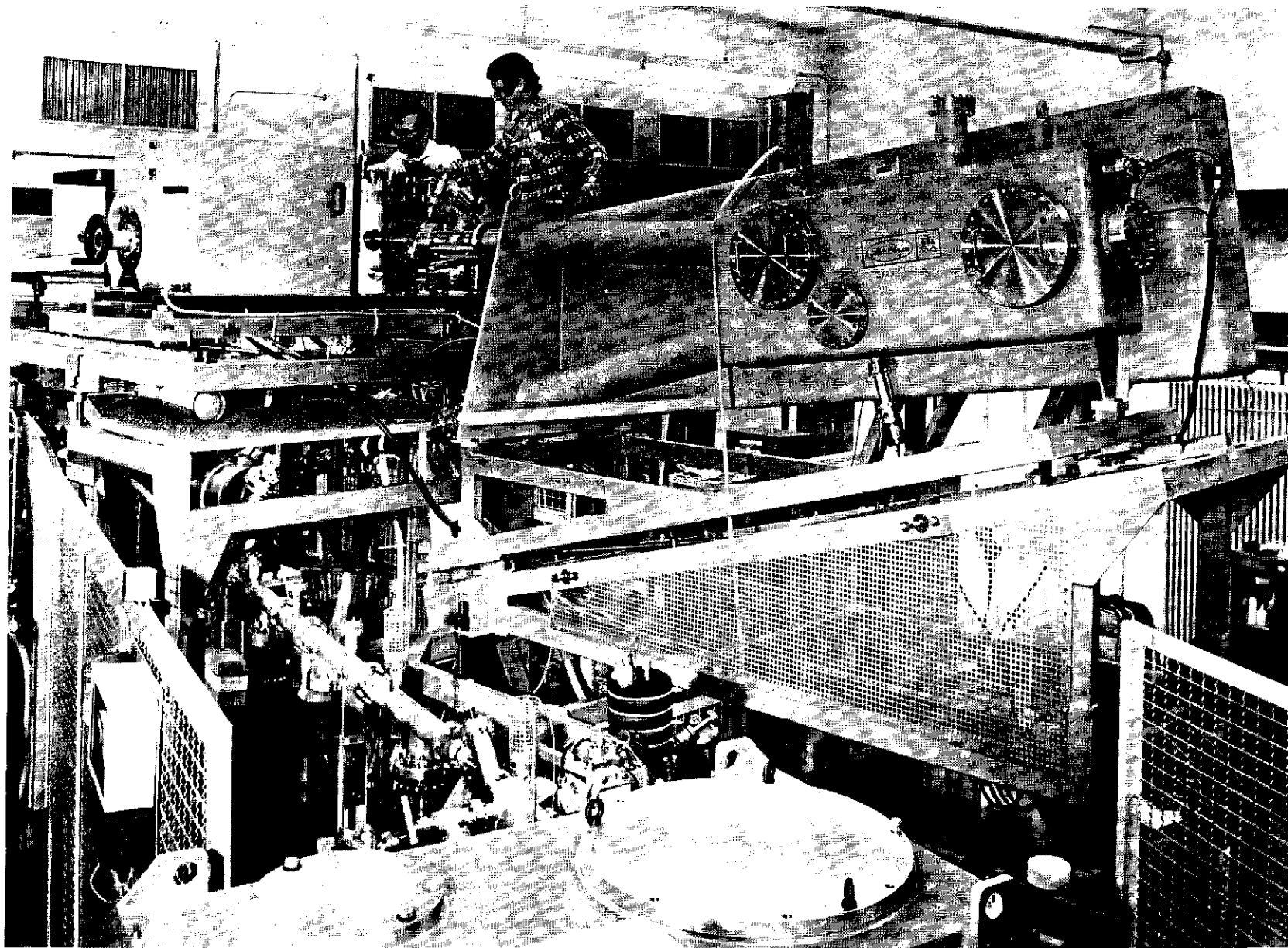


Fig. 3

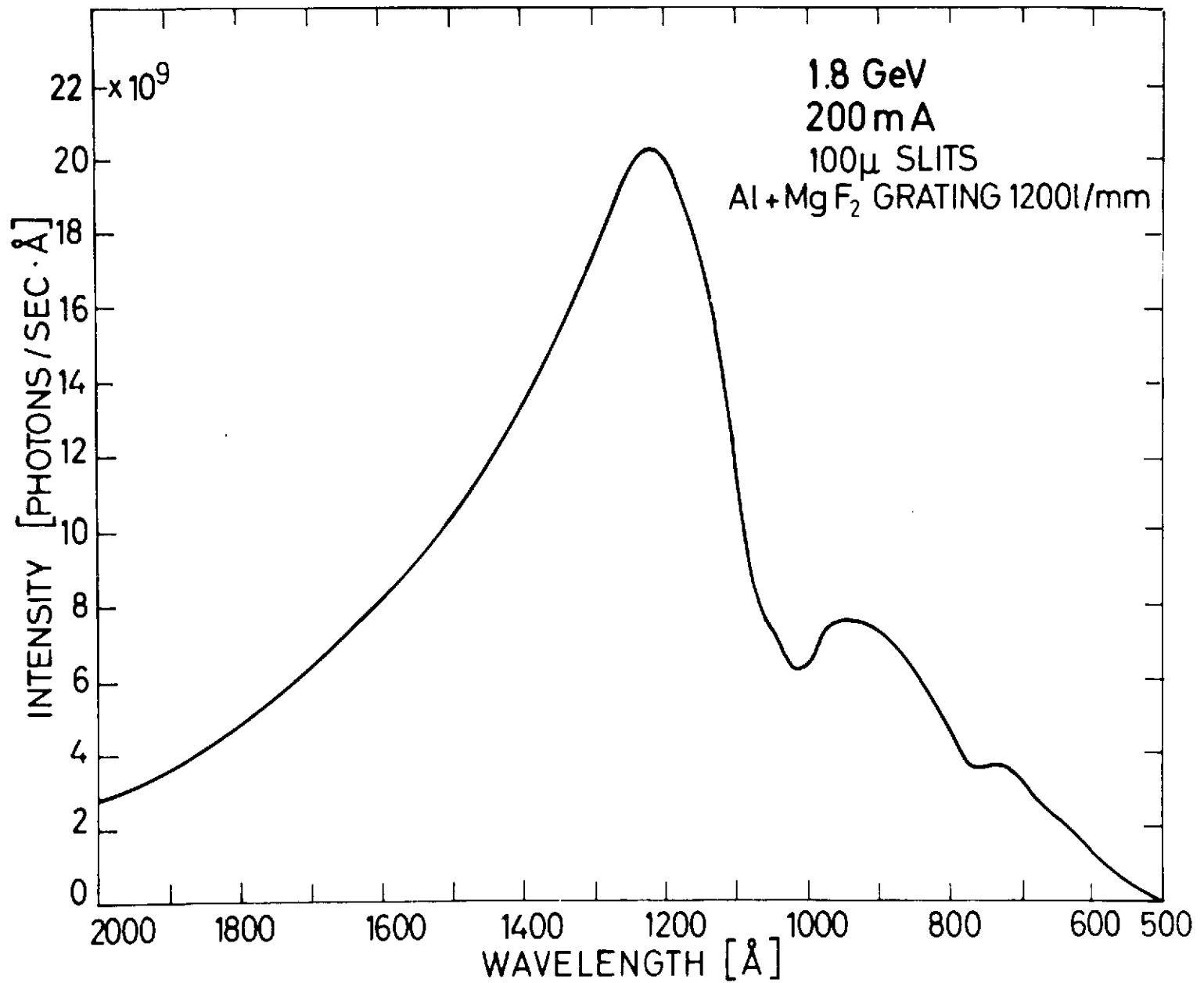
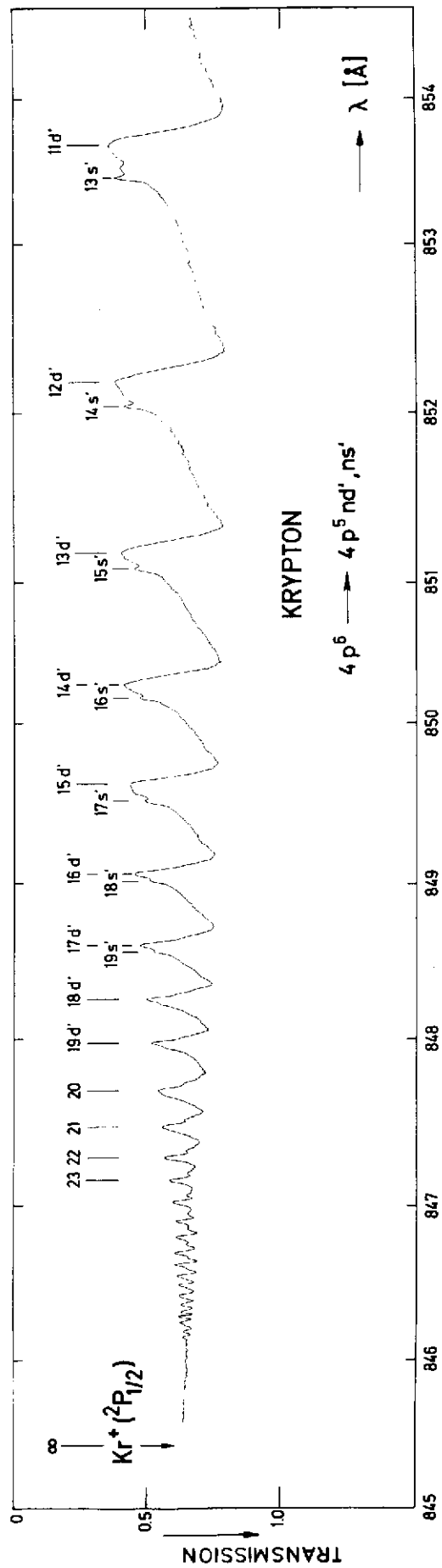


Fig. 4

DESY

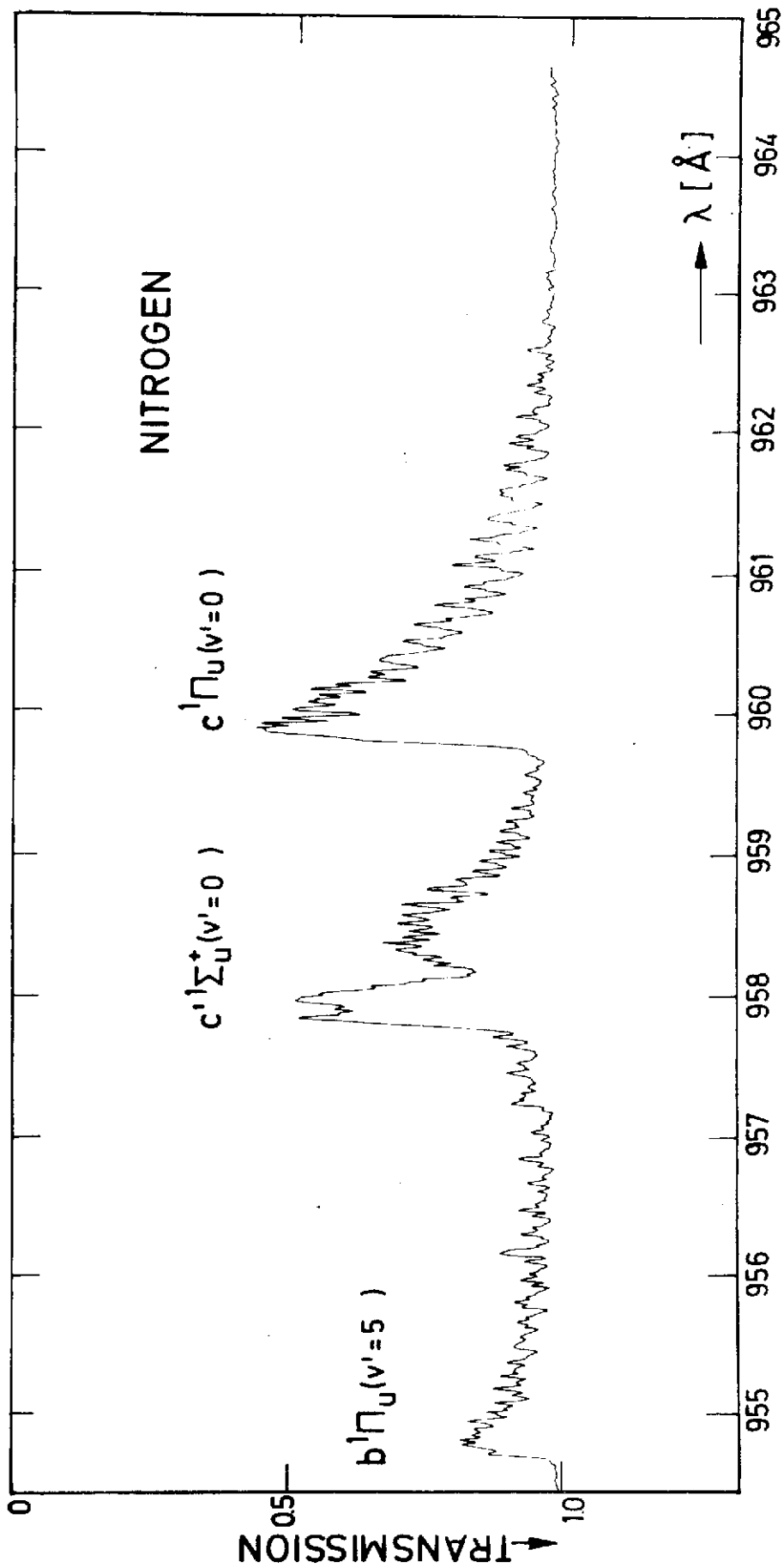
23834



DES Y

23832

Fig. 5



DESY

23833

Fig. 6

